

Optimal Step-Size Technique for Frequency-Domain and Partition-Block Adaptive Filters for PEM based Acoustic Feedback Cancellation

S. Siva Prasad* and C.B. Rama Rao

Department of ECE, National Institute of Technology, Warangal - 506004, India

*E-mail: sivaphd.nitw@gmail.com

ABSTRACT

The adaptive filtering approach has been commonly used to perform acoustic feedback cancellation (AFC) in digital hearing-aids due to its reliable performance and feasibility. Because the loudspeaker and microphone are close together in hearing aids, the corresponding signals are highly correlated, resulting in biased estimation if adaptive filters are used. This problem can be addressed with the help of the decorrelation prefilter by incorporating the Prediction Error Method (PEM) technique into AFC. Frequency-Domain Adaptive Filters (FDAF) are preferable over the time-domain implementation to achieve better performance in terms of convergence and computational complexity. In addition, Partition-Block Frequency-Domain Adaptive Filters (PBFDAF) offers low processing delay. However, because of their fixed step-size, there is a trade-off between initial convergence and steady-state misalignment in the widely used frequency-domain algorithms. While Variable Step-Size (VSS) algorithms can help with this issue, VSS techniques for frequency-domain algorithms have not been extensively studied in the context of PEM-AFC. Hence, in this paper, we presented an Optimal Step-Size (OSS) technique for both the FDAF-PEM_AFC and PBFDAF-PEM_AFC algorithms to simultaneously accomplish fast convergence and minimal steady-state error. A Feedback Path Change Detector (FPCD) was also incorporated into the proposed algorithms to address the problem of convergence in non-stationary feedback paths. The results of simulations show that the proposed algorithms are clearly superior, and they are encouraging.

Keywords: Optimum step-size; Frequency-domain adaptive filter; Partition-block adaptive filter; Hearing aids; Acoustic feedback cancellation; Prediction error method

NOMENCLATURE

		$U(l)$	Loudspeaker signal vector in frequency-domain
n_w	Length of the adaptive filter	$\hat{H}(q,l)$	Source signal model
N	FFT size	$\hat{A}(q,l)$	Prediction filter
R	FFT frame shift	$u_j(l)$	Prewhitened loudspeaker signal vector
m	Frequency bin number	$s_j(l)$	Prewhitened microphone signal vector
w	Actual acoustic feedback path	$e_j(l)$	Prewhitened error signal
\hat{w}	Adaptive filter weight vector in time-domain to estimate the acoustic path	$U_j(l)$	Prewhitened loudspeaker signal vector in frequency-domain
\hat{W}	Weight vector of frequency-domain adaptive filter	$E_j(l)$	Prewhitened error signal vector in frequency-domain
\hat{W}_p	Weight vector of partition-block frequency domain adaptive filter	$\mu_m(l)$	Optimal step-size of m^{th} frequency bin
P	No. of partition-blocks of filter weight vector	$\delta_m(l)$	System distance of m^{th} frequency bin
$s(n)$	Microphone signal vector of length N	$Mis(l)$	Misalignment error of l^{th} frame
$e(n)$	Error signal	$MSG(l)$	Maximum achievable stable gain of l^{th} frame
$\hat{W}_{(n)}$	Weight vector of adaptive filter		
$\hat{W}_{(l)}$	Frequency-domain weight vector		

$\Phi_{u_f, p}(l)$	Elements of PSD matrix of the prefiltered loudspeaker signal
$\Phi_{s, m}(l)$	Elements of PSD matrix of the desired signal
$\Phi_{e_f, m}(l)$	Elements of PSD matrix of the prefiltered error signal
$\Lambda(l)$	PSD matrix of loudspeaker signal
$\mu_{p, m}(l)$	Optimal step-size of m^{th} frequency bin for p^{th} partition
$\delta_{p, m}(l)$	Optimal step-size of m^{th} frequency bin for p^{th} partition

Note: The variables mentioned in smaller case letters denote time-domain; capital case letters represents frequency domain variables; bold letters represent signal vectors.

ABBREVIATIONS

AFC	Acoustic Feedback Canceller
FDAF	Frequency-Domain Adaptive Filter
PBFDAF	Partition-Block Frequency Domain Adaptive Filter
PEM	Prediction-Error Method
OSS	Optimal Step-Size
FSS	Fixed Step-Size
FFT	Fast Fourier Transform
LMS	Least Mean Square
PSD	Power Spectral Density
AEC	Acoustic Echo Cancellation
FPCD	Feedback Path Change Detector
LS	Loudspeaker
Mis	Misalignment
MSG	Maximum Stable Gain
AIR	Acoustic-Impulse Response
PESQ	Perceptual Evaluation of Speech Quality

1. INTRODUCTION

In digital hearing-aids, acoustic feedback is a serious issue¹, it is the main cause of howling, whistling, and screeching sounds. It occurs when the input signal at the microphone's input signal is acoustically coupled with the loudspeaker signal. As the acoustic coupling increases, the desired signal degrades quickly and causes annoying howling. There are numerous strategies for Acoustic Feedback Cancellation (AFC), but adaptive filtering is most effective, which involves the continuous estimation of the acoustically coupled signal and then subtracted from the microphone signal.² The primary disadvantage of this strategy is that the output signal from the loudspeaker is a combination of feedback and input signals.³⁻⁴ Since there is a correlation present among the desired and loudspeaker signals, the feedback signal, which is a part of loudspeaker signal, is also correlated with the desired source signal. As a result of this correlation, the adaptive filter may experience a problem with estimation bias.

The Prediction-Error Method (PEM) is commonly employed in AFC for estimating an unbiased model of the

acoustic path by decorrelating the signals in the feedback loop with the help of a pre-whitening filter.⁴⁻⁷ Figure 1, illustrates the PEM-AFC, w represents the actual acoustic path between microphone and loudspeaker, \hat{w} represents the estimated acoustic path in feedback loop, which is continuously estimated by an adaptive filter, and G represents the hearing-aid gain with a forward delay of d_G .

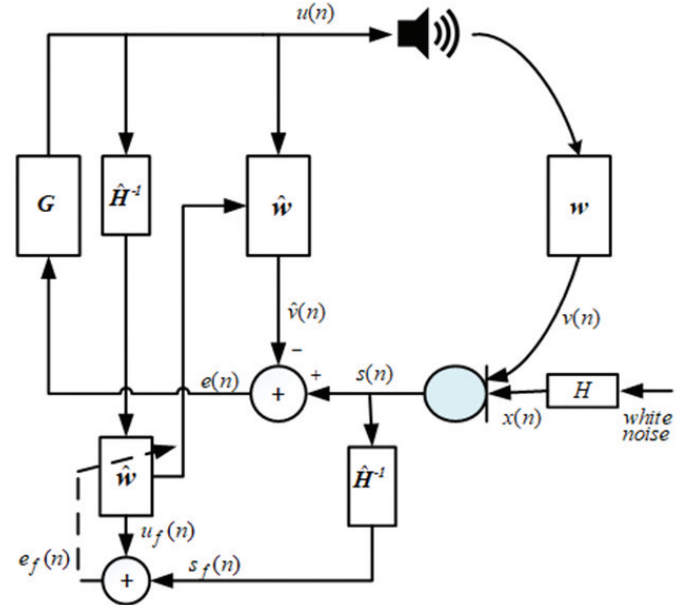


Figure 1. PEM-AFC system.

The design of an effective adaptive feedback controller demands an unbiased estimation of acoustic path, good steady-state performance, and the adaptive algorithm's convergence rate.⁸⁻⁹ The LMS algorithm has a low convergence rate for colored signals and a high computational complexity when modeling an acoustic path with more number of filter weights⁵. The frequency-domain version of LMS algorithm has the advantage of being less computationally complex and obtaining faster convergence than the time-domain implementation.¹⁰⁻¹¹ Further improvement in convergence rate is achieved by estimating the feedback path using block Frequency Domain Adaptive Filters (FDAF). To reduce the delay associated with block processing in FDAF, PBFDAF algorithm is recommended. However, the performance of FDAF and PBFDAF algorithms is heavily reliant on fixed step-size(FSS) selection.¹² To address the limitations of FSS approach, we often use variable step-size techniques, wherein the step-size changes over time depending on the state of algorithm.

An optimal step-size (OSS) approach for the FDAF and PBFDAF algorithms for AEC configuration has been developed by Yang, *et al.*^{12,16} and we have briefly studied OSS technique for PBFDAF algorithm for AFC system in Prasad, *et al.*¹³ This paper presents a comprehensive study of the OSS approach for FDAF and PBFDAF algorithms implemented for PEM-AFC configuration, and these are compared in terms of convergence, complexity analysis, and output speech quality.

The contents of this article are organised in the following manner: modelling of PEM-AFC configuration and implementation of fixed step-size FDAF-PEM-AFC and PBFDAF-PEM-AFC algorithms in Section 2, while

Section 3 discusses the proposed frequency-domain optimal step-size algorithms for PEM-AFC. Section-4 and section-5 discuss about simulation results and computational complexity analysis of proposed algorithms, respectively, and the final section provides the work's conclusion.

2. FIXED STEP-SIZE (FSS) ALGORITHMS FOR PEM-AFC SYSTEM

2.1 Modelling of PEM-AFC System

The PEM-AFC illustrated in Fig. 1 uses the benefits of source signal modelling by employing a PEM-based pre-whitening technique,¹⁵ which significantly minimizes the correlation among the signals in feedback loop. This decorrelation facilitates a reduction in the bias of the estimated feedback path, resulting in a more efficient feedback cancellation. The model $H(q,l)$ that generates the source signal $x(n)$ is assumed to be autoregressive (AR) and time-varying. Hence, using the linear-prediction technique, $\hat{H}(q,l)$ can be estimated using the Levinson-Durbin algorithm¹⁵ and, from the condition $\hat{H}(q,l)\hat{A}(q,l)=1$, the pre-whitening filter $\hat{A}(q,l)$ is equal to inverse of $\hat{H}(q,l)$. The mathematical modeling of the PEM-AFC² is described below:

$$s(n) = \mathbf{u}^T(n) \mathbf{w}_o(n) + x(n) \quad (1)$$

$$e(n) = s(n) - \mathbf{u}^T(n) \hat{\mathbf{w}}(n) \quad (2)$$

where $\mathbf{w}_o(n)$ is actual feedback path, $\hat{\mathbf{w}}(n) = [w_0, \dots, w_{n_w-1}]^T$ denotes an adaptive filter of length n_w , $\mathbf{s}(n) = [s(n), \dots, s(n-n_w+1)]$ represents microphone signal vector, $\mathbf{e}(n)$ denotes error signal (\cdot^T stands for transpose of a matrix, $\mathbf{u}(n) = [u(n), \dots, u(n-n_w+1)]^T$ represents loudspeaker signal, and $x(n)$ denotes combination of desired signal and the background noise.

To model the problem in the frequency domain, we need to change from the time-instant n to time-frame index l ; assume FFT size is N , discrete frequency index m and the frame shift R . A good choice for R and N is $R = \frac{N}{2}$; $N = 2R$ ¹². The loud-speaker signal frame at time l of length N -samples is $\mathbf{u}(l) = [u(lR-N+1), \dots, u(lR-1), u(lR)]^T$, and the microphone signal frame of length R samples is $\mathbf{s}(l) = [s(lR-R+1), \dots, s(lR-1), s(lR)]^T$.

$$\mathbf{U}(l) = \text{diag}\{\mathcal{F}_N \mathbf{u}(l)\} \quad (3)$$

The estimating acoustic feedback $\hat{\mathbf{W}}(l)$ path is specified in the frequency-domain by, $\hat{\mathbf{W}}(l) = \mathcal{F}_N [\hat{\mathbf{W}}^T(l), \mathbf{0}_{1 \times R}]^T = [\hat{W}_0(l), \dots, \hat{W}_{N-1}(l)]^T$ where $\mathbf{0}_{1 \times R}$ is a zero vector.

The estimated feedback signal and error-signal, in each time-frame are obtained from the below equations respectively,

$$\tilde{\mathbf{s}}(l) = \mathcal{F}_N^{-1} \{\mathbf{U}(l) \hat{\mathbf{W}}(l)\} \quad (4)$$

$$e(l) = s(l) - \hat{s}(l) \quad (5)$$

where $\hat{s}(l)$ is last frame of $\hat{s}(l)$, which is obtained from eq (4). From the error signal in Eqn. (5), we can estimate $\hat{H}(q,l)$ and prediction filter $\hat{A}(q,l)$ using Levinson-Durbin algorithm as given below,

$$\hat{A}(q, l+1) = \text{levinson-durbin}\{e(l); e(l-1)\} \quad (6)$$

2.2 PEM-AFC System using FSS-FDAF Algorithm

This section describes the FDAF algorithm for the PEM-AFC configuration.^{2,4,17} The pre-whitened signal vectors of $\mathbf{u}_f(l)$ and $\mathbf{s}_f(l)$ are obtained by filtering with $\hat{A}(q,l)$. Thus, the pre-whitened loud-speaker and microphone signal vectors are written as,

$$\mathbf{u}_f(l) = \begin{bmatrix} \hat{A}(q,l)u(lR-N+1) \\ \vdots \\ \hat{A}(q,l)u(lR) \end{bmatrix} = [u_f(lR-N+1) \dots u_f(lR-1), u_f(lR)]^T \quad (7)$$

$$\mathbf{s}_f(l) = \begin{bmatrix} \hat{A}(q,l)s(lR-R+1) \\ \vdots \\ \hat{A}(q,l)s(lR) \end{bmatrix} = [s_f(lR-R+1) \dots s_f(lR-1), s_f(lR)]^T \quad (8)$$

The pre-whitened loudspeaker signal $\mathbf{u}_f(l)$ is converted to frequency domain by N point FFT matrix \mathcal{F}_N and associated diagonal matrix is obtained with $\text{diag}\{\cdot\}$ operator, as below,

$$\mathbf{U}_f(l) = \text{diag}\{\mathcal{F}_N \mathbf{u}_f(l)\} = \text{diag}\{[U_{f0}(l), U_{f1}(l), \dots, U_{f(2N-1)}(l)]^T\} \quad (9)$$

The FFT representation of prefiltered microphone signal frame $\mathbf{s}_f(l)$ is obtained by $\mathbf{s}_f(l) = \mathcal{F}_N [\mathbf{0}_{1 \times N}, \mathbf{s}_f(l)]$. Thus, the prefiltered error vector in the frequency domain, is written as

$$\mathbf{E}_f(l) = \mathbf{S}_f(l) - \mathcal{G}^{01} \mathbf{U}_f(l) \hat{\mathbf{W}}(l) \quad (10)$$

where, $\mathcal{G}^{01} = \mathcal{F} \begin{bmatrix} \mathbf{0}_R & \mathbf{0}_R \\ \mathbf{0}_R & \mathbf{I}_R \end{bmatrix} \mathcal{F}$, is the windowing matrix which makes the first R samples to zeros. Hence, the overlap-save constrained FDAF algorithm's weight updating equation of PEM_AFC is written as:

$$\hat{\mathbf{W}}(l+1) = \hat{\mathbf{W}}(l) + \mathcal{G}^{10} \mu \Lambda^{-1}(l) \mathbf{U}_f^H(l) \mathbf{E}_f(l) \quad (11)$$

where, μ is the fixed step-size, $\mathcal{G}^{10} = \mathcal{F} \begin{bmatrix} \mathbf{I}_R & \mathbf{0}_R \\ \mathbf{0}_R & \mathbf{0}_R \end{bmatrix} \mathcal{F}^{-1}$

which makes the last R samples to zero and,

$\Lambda(l) = \text{diag}\{[\Phi_{u_f,0}(l), \dots, \Phi_{u_f,2N-1}(l)]^T\} = E[\mathbf{U}_f^H(l) \mathbf{U}_f(l)]$, is the loudspeaker signal's PSD matrix, which helps to make the algorithm's tracking behaviour better. The PSD of pre-whitened

loudspeaker signal can be determined by smoothing the FFT coefficients recursively as,

$$\hat{\Phi}_{u_f,m}(l) = \lambda \hat{\Phi}_{u_f,m}(l-1) + (1-\lambda) |U_{f,m}(l)|^2 \quad (12)$$

where, $m = 0, 1, 2, \dots, 2N-1$, represents frequency-bin number and $0 < \lambda < 1$ is the smoothing-factor.

2.3 PEM-AFC System using FSS-PBFDAF

Algorithm

In the PBFDAF algorithm, filter weights of the estimating acoustic path \hat{w} are divided into P smaller sets of weight vectors as \hat{w}_p , where $p = 0, 1, \dots, P-1$. The weight vector of p^{th} subfilter is $\hat{w}_p(l) = [\hat{w}(pN), \dots, \hat{w}(pN + N - 1)]^T$ with no. of taps $N = n_w / P$. Thus, for PBFDAF-PEM-AFC,^{2,18} the pre-whitened error signal is calculated by,

$$e_f(l) = s_f(l) - \sum_{p=0}^{P-1} \mathbf{u}_{f,p}^T(l) \hat{w}_p(l) \quad (13)$$

where $\mathbf{u}_{f,p}(l) = [u_f(l-pN), \dots, u_f(l-(p+1)N+1)]^T$

The smaller convolutions in Eqn. (13) can be carried out effectively in frequency-domain using FFT. The pre-whitened loudspeaker signal and the weight vector corresponding to the p^{th} partition in the frequency-domain are given by the following equations respectively,

$$U_{f,p}(l) = \text{diag}\{\mathcal{F}\mathbf{u}_{f,p}(n)\} = \text{diag}\{[U_{f,p(0)}(l), \dots, U_{f,p(2N-1)}(l)]^T\} \quad (14)$$

$$\hat{w}_p(l) = \mathcal{F}[\hat{w}_p(l), \mathbf{0}_{1 \times N}]^T = [\hat{W}_{l,0}(l), \dots, \hat{W}_{p,2N-1}(l)]^T \quad (15)$$

where $\mathbf{0}_{1 \times N}$ is a zero vector. The pre-whiten error signal vector in frequency-domain representation is

$E_f(l) = [E_{f,0}(l), \dots, E_{f,2N-1}(l)]^T$ and it can be obtained by,

$$E_f(l) = S_f(l) - \mathcal{G}^{01} \sum_{p=0}^{P-1} U_{f,p}(l) \hat{w}_p(l) \quad (16)$$

where, $S_f(l) = \mathcal{F}[0_{1 \times N}, s_f(lN), \dots, s_f((l+1)N-1)]^T$ is pre-

whiten microphone signal and $\mathcal{G}^{01} = \mathcal{F} \begin{bmatrix} \mathbf{0}_N & \mathbf{0}_N \\ \mathbf{0}_N & \mathbf{I}_N \end{bmatrix} \mathcal{F}^{-1}$. Thus,

the update equation of PBFDAF algorithm for PEM-AFC is expressed by,

$$\hat{w}(l+1) = \hat{w}_p(l) + \mathcal{G}^{\lambda 10} \mu \Lambda_p(l) U_{f,p}^H(l) E_f(l) \quad (17)$$

where $(\cdot)^H$ indicates matrix hermitian, is

the fixed step size, $\mathcal{G}^{10} = \mathcal{F} \begin{bmatrix} \mathbf{I}_N & \mathbf{0}_N \\ \mathbf{0}_N & \mathbf{0}_N \end{bmatrix} \mathcal{F}^{-1}$, and

$\hat{E}_p = \text{diag}\{\Phi_{u_f,p}(0), \dots, \Phi_{u_f,p}(2N-1)\} = E[U_{f,p}^H(l) U_{f,p}(l)]$ is PSD of

pre-whiten load-speaker signal. The PSD of pre-whitened loudspeaker can be estimated recursively as,

$$\hat{\Phi}_{u_{f,p},m}(l) = \lambda \hat{\Phi}_{u_{f,p},m}(l-1) + (1-\lambda) |U_{f,p,m}(l)|^2 \quad (18)$$

where $m = 0, 1, 2, \dots, 2N-1$, represents frequency bin number and λ is the smoothing factor, $0 < \lambda < 1$.

3. PROPOSED OPTIMAL STEP SIZE (OSS) ALGORITHMS FOR PEM-AFC

3.1 OSS Technique for FDAF Algorithm in the Context of PEM-AFC

The step-size of the FDAF algorithm for PEM-AFC is fixed in the weight update Eqn. (11), which results in either a slower convergence rate for small step-sizes or higher steady-state error with large step-sizes. To overcome this trade-off, we proposed an approach for determining the OSS for FDAF-PEM-AFC algorithm. The methodology for estimating the OSS for the FDAF algorithm in the case of AEC is discussed by Yang,¹² *et al.*, and we are using a similar approach for proposing OSS-FDAF-PEM-AFC algorithm. To describe variable step-size FDAF-PEM-AFC algorithm, replace the fixed step-size μ in the weight update Eqn. (11) with variable step-size $\mu_m(l)$, and consequently, the equation for filter weight update is written as:

$$\hat{w}(l+1) = \hat{w}(l) + \mathcal{G}^{10} \mu_m(l) \Lambda^{-1}(l) f^H E_f(l) \quad (19)$$

where $\mu_m(l) = \text{diag}\{\mu_0(l), \dots, \mu_{2N-1}(l)\}^T$, the suffix denotes m^{th} frequency-bin. The following assumptions are made to obtain the expression for optimal step-size:

(i) We assume that the weight vector is random, zero-mean, and follows first-order simplified Markov model.⁵⁻¹⁹ In frequency-domain, weight vector can be approximated by the following equation, where $H(l)$ is uncorrelated with filter weights and loudspeaker signal,

$$w_o(l+1) = w_o(l) + H(l) \quad (20)$$

(ii) In Eqn. (19), the frequency-domain weight vector $\hat{w}_p(l)$ is statistically independent to $U_f(l)$ and $S_f(l)$.

(iii) $E[U_{f,i}(l) U_{f,j}^*(l)] = 0$ for $i \neq j$.

We get an equation for system distance $\delta_m(l)$ by using the above assumptions and performing the convergence analysis as described by Yang¹², *et al.*, but this system distance is minimum if the step-size is optimal, so we get the OSS by equating $\frac{\partial \delta_m(l+1)}{\partial \mu_m(l)} = 0$. The expressions for OSS and system distance were obtained as follows:

$$\mu_m(l) = \frac{\Phi_{u_f,m}(l) \delta_m(l)}{\Phi_{u_f}(l) \delta_m(l) + 2\Phi_{x,m}(l)} \quad (21)$$

$$\delta_m(l+1) = \left(1 - \frac{\mu_m(l)}{4}\right) \delta_m(l) + \Theta_m(l) \quad (22)$$

where, $\Theta_m(l) = E(|H_m(l)|^2)$, is a measure of the acoustic path's impulse response variability. When $\Theta_m(l)$ is not considered in Eqn (22), $\delta_m(l)$ has a tendency to reach zero or lower value as time increases, it results in good steady state performance but poor tracking of the system when an abrupt change in feedback path occurs, $\Theta_m(l)$, should have larger value to enable fast tracking. Hence, this parameter has an effect on both tracking and steady-state misalignment. To achieve a good trade-off, it can be estimated by the below expression as given in²⁰,

$$\Theta_m(l) = |\hat{W}_m(l+1) - \hat{W}_m(l)|^2 \quad (23)$$

Since, the algorithm's convergence performance is relatively insensitive, system distance is initialized with a constant. Additionally, when the filter converges to a certain degree, Eqn (22) requires the estimation of the source signal PSD, which can be approximated to the PSD of the pre-filtered error signal. As a result, the PSD estimation of the source signal is $\Phi_{x,m}(l) \approx \Phi_{e_f,m}(l)$, and thus PSD estimation of the PEM error signal is.

$$\Phi_{e_f,m}(l) = \alpha \Phi_{e_f,m}(l-1) + (1-\alpha) |E_{f,m}(l)|^2 \quad (24)$$

where, α is smoothing factor between 0 and 1.

Although the proposed OSS_FDAF-PEM-AFC has fast convergence with minimal steady-state error, its tracking capability for changes in the feedback path is limited because of the decreasing nature of system distance with respect to time as in Eqn. (22), with time and also when the feedback path changes noise PSD in Eqn. (24) is overestimated. As a result, the step size from Eqn. (21), becomes extremely small, and the algorithm's behavior becomes unpredictable when the feedback path changes. To overcome this reconvergence problem, a feedback path change detection logic¹⁴ has been added to the proposed algorithm.

3.2 OSS Technique for PBFDAF Algorithm in the Context of PEM-AFC

Similar to the previous section, to represent the OSS weight update in PBFDAF-PEM-AFC, step-size μ in Eqn. (17) is replaced with variable step-size $\mu_{p,m}(l)$, for p^{th} partition and m^{th} frequency bin, and the weight vector of the next frame is obtained by,

$$\hat{W}_p(l+1) = \hat{W}_p(l) + \mathcal{G}^{10} \mu_{p,m}(l) \Lambda^{-1}(l) U_{fp}^H E_f(l) \quad (25)$$

where $\mu_{p,m}(l) = \text{diag}\{\mu_{p,0}(l), \dots, \mu_{p,2N-1}(l)\}^T$. The following assumptions are made to obtain the expression for optimal step-size: (i) the vectors $U_{fp}(l)$ and $x(l)$ are stationary, zero-mean, and statistically independent random processes; (ii) $U_{fp}(l)$ and

$x(l)$ are statistically independent to each partition's weight vector $\hat{W}_p(l)$; (iii) $E[U_{fi}(l)U_{fj}^*(l)] = 0$ for $i \neq j$. With the above assumptions and by performing the convergence analysis¹⁶, we obtain an equation for system distance $\delta_{p,m}(l)$ but this system distance is minimum if the step-size is optimal, so,

we can obtain the OSS by equating $\frac{\partial \delta_{p,m}(l+1)}{\partial \mu_{p,m}(l)} = 0$. By solving

this derivative, we obtain the expressions for OSS and system distance as follows,

$$\mu_{p,m}(l) = \frac{\Phi_{u_f,m}(l) \delta_{p,m}(l)}{\Phi_{u_f,m}(l) \left[\delta_{p,m}(l) + \frac{1}{2} \sum_{p=0, m \neq p}^{P-1} \delta_{p,m}(l) \right] + 2\Phi_{x,m}(l)} \quad (26)$$

$$\delta_{p,m}(l+1) = \left[1 - \frac{\mu_{p,m}(l)}{2} + \frac{\mu_{p,m}^2(l)}{4} \right] \delta_{p,m}(l) + \frac{1}{8} \mu_{p,m}^2(l) \times \sum_{p=0, m \neq p}^{P-1} \delta_{p,m}(l) + \frac{1}{2} \mu_{p,m}^2(l) \frac{\Phi_{x,m}(l)}{\Phi_{u_f,m}(l)} \quad (27)$$

As described in previous section, the PSD estimation of noise have been approximated by, $\Phi_{x,m}(l) \approx \Phi_{e_f,m}(l)$ and the PSD of PEM error-signal can be estimated by,

$$\Phi_{e_{fp},m}(l) = \alpha \Phi_{e_{fp},m}(l-1) + (1-\alpha) |E_{fp,m}(l)|^2 \quad (28)$$

where $0 < \alpha < 1$ is the smoothing factor. Here also to overcome the reconvergence problem, FPCD logic as discussed in previous section, has to be included in this proposed OSS-PBFDAF-PEM-AFC algorithm.

4. SIMULATION RESULTS

This section discusses the simulation results of proposed algorithms OSS-FDAF-PEM-AFC and OSS-PBFDAF-PEM-AFC. The developed algorithms are compared against the FDAF-PEM-AFC, PBFDAF-PEM-AFC algorithms, using the fixed step-size for adaptation. We assumed one fixed step-size to be a higher value and the other to be a lower value in our simulations because higher step-size provides fast tracking and lower step-size provides good steady-state performance. In this study, three metrics are used to compare the algorithms, they are Misalignment (Mis), achievable maximum stable gain (MSG) and perceptual evaluation of speech quality (PESQ). The Misalignment²⁰ is an estimation error, which is defined as the normalized value of difference between the actual feedback path and estimated path, often expressed in decibels (dB).

$$\text{Mis}(l) = 20 \log_{10} \left\| \frac{\mathbf{w}_r(l)}{\mathbf{w}_o(l)} \right\| \quad (29)$$

where $\mathbf{w}_r(l) = \mathbf{w}_o(l) - \hat{\mathbf{w}}(l)$. MSG²⁰ is the maximum stable

amplification that can be attained at a given time when the forward gain is constant.

$$MSG(l) = -20 \log_{10} [\max |w_r(l)|] \quad (30)$$

The effectiveness of algorithms have been compared based on assessment of output speech quality using PESQ²¹ score. The PESQ measure takes a value between -0.5 and 4.5, where -0.5 means that the quality of speech is very poor and a score of 4.5 means the speech quality is best. To measure PESQ score of an AFC system, the incoming signal $x(n)$ is considered as reference signal and the loudspeaker signal $u(n)$ as test signal.¹¹

The acoustic paths used in the simulation study are taken from,²⁰⁻²¹ two different acoustic paths are considered for our study. For the first half of the simulation time, the acoustic path in the free field i.e., AIR1 is used, and for the second half, we employ AIR2, which is an acoustic path when an object like a mobile phone is kept near the ear. Fig. 2 depicts the amplitude response of two feedback paths

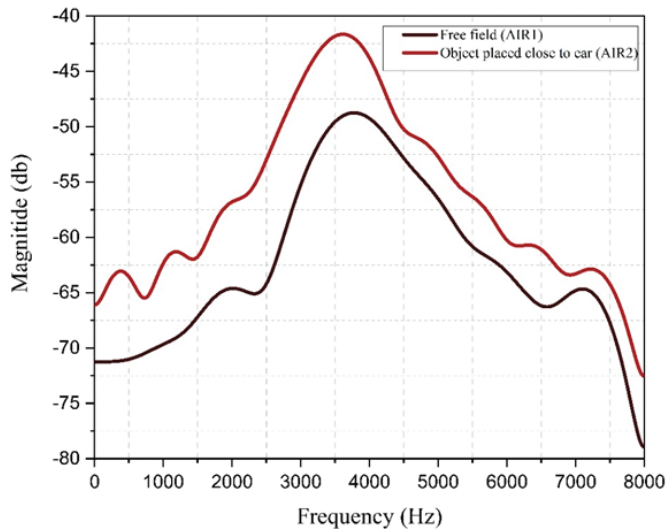


Figure 2. Frequency characteristics of the acoustic feedback paths.

with respect to frequency. The misalignment and MSG plots are the average of ten different simulation runs, using ten different speech signals. Each speech signal lasts sixty seconds and is concatenated with female and male speech signals extracted from the TIMIT database. The sample frequency is set at 8 kHz. For all the simulations the following parameters are

used: $n_w = 80$, $R = \frac{n_w}{P}$ where $P=1$ for FDAF and $P=4$ for PBFDAF algorithms, $N = 2R$, $\delta_c = 1.0$, $\lambda = 0.85$, $\alpha = 0.9$, $\beta = 0.75$. Two different fixed step-sizes are considered, one is low step value $\mu = 0.001$, which can provide lower steady state error, and the other one is $\mu = 0.02$ which gives faster tracking. Fig. 3 and Fig. 4, provides the comparison of misalignment and MSG of the proposed algorithms OSS algorithms with fixed step-size FDAF and PBFDAF algorithms for PEM-AFC. The plot demonstrates that the proposed algorithms have a higher rate of convergence and a lower steady-state error than the FSS algorithms. Although the OSS-FDAF algorithm has slightly

faster convergence rate of the two proposed algorithms, their steady-state performance is very similar. Moreover, when the feedback path changes from AIR1 to AIR2 at 30 seconds, the proposed approaches as shown in Fig. 5 and Fig. 6, are capable of tracking the shift accurately.

The output speech quality is assessed with the help of PESQ to analyse the performance of AFC algorithms. The average PESQ values are reported in Table 1 for ten different input speech signals to the AFC system. The PESQ measure shows that OSS algorithms outperform FSS methods, and among the optimal step-size algorithms, OSS-PBFDAF-PEM-AFC algorithm marginally outperforms the OSS-FDAF-PEM-AFC method in terms of PESQ, which is owing to low processing delay of OSS-PBFDAF-PEM-AFC.

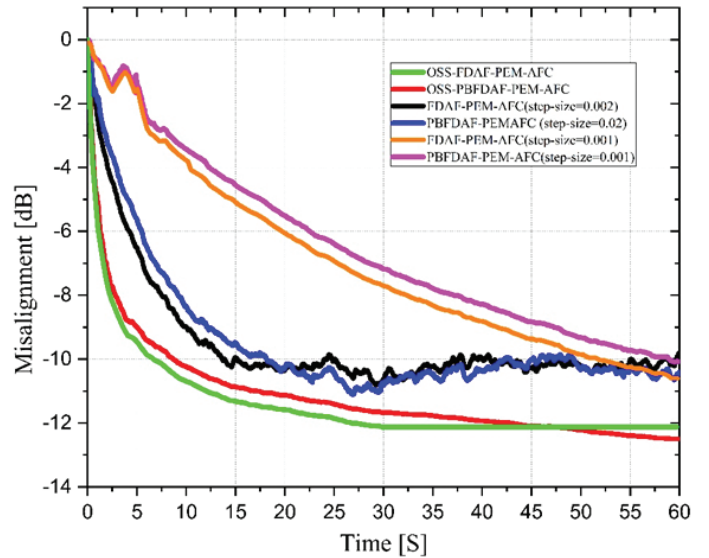


Figure 3. Misalignment comparison of proposed algorithms OSS-FDAF-PEM-AFC and OSS-PBFDAF-PEM-AFC, with FSS algorithms.

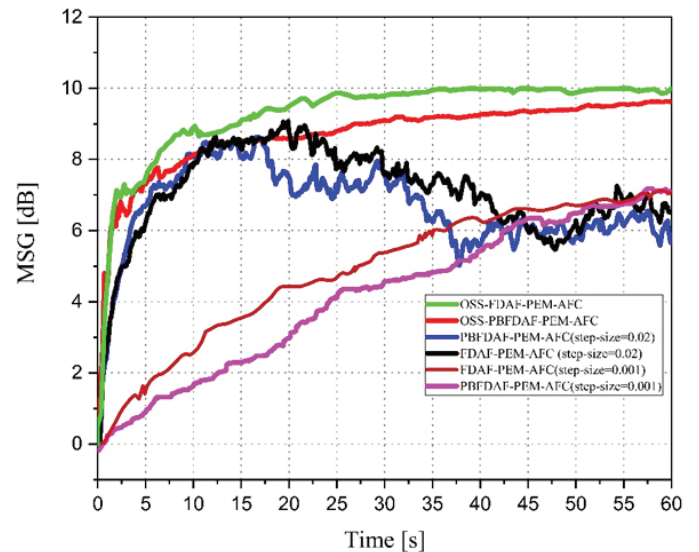


Figure 4. MSG comparison of proposed OSS algorithms with FSS algorithms.

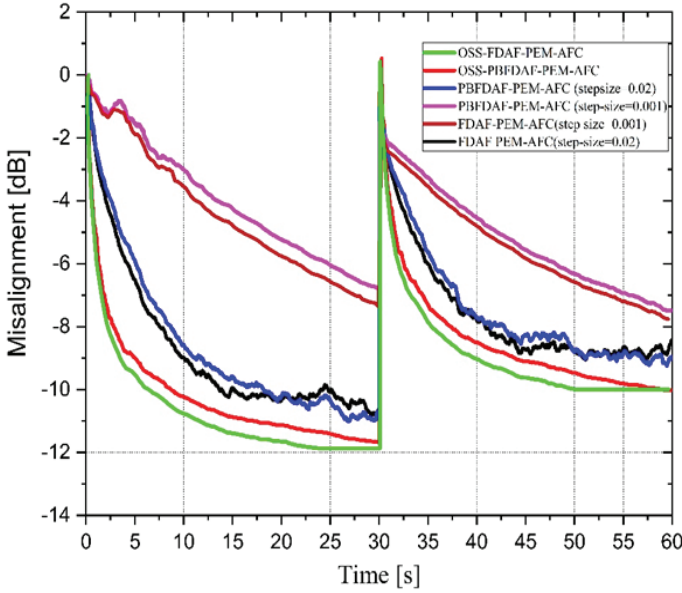


Figure 5. Misalignment comparison of proposed OSS algorithms with FSS algorithms when the feedback path changes at 30s from AIR1 to AIR2.

5. COMPLEXITY ANALYSIS

The complexity analysis of the proposed OSS-FDAF-PEM-AFC and OSS-PBFDFAF-PEM_AFC algorithms and their comparison with the fixed step size FDAF and PBFDFAF algorithms for PEM-AFC is discussed in this section. The number of real multiplications required for each output sample is used to compare the computational complexity of different algorithms. We made the following assumptions: A real division and multiplication are both equally complex; each N point FFT/IFFT calculation requires $N \log_2 N$ multiplications, the Levinson-Durbin method has a complexity of $n_A^2 + (5 + N)n_A + N$ multiplications²¹, where n_A is the length of prediction-filter. The complexity analysis of the OSS-FDAF-PEM-AFC and OSS-FDAF-PEM-AFC algorithms are provided in the Table 1 and Table 2 respectively.

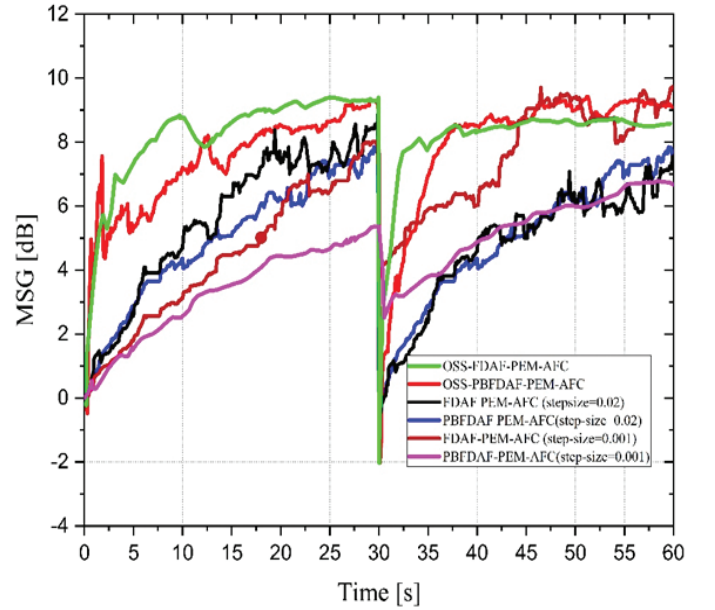


Figure 6. MSG comparison of proposed OSS algorithms with FSS algorithms when the feedback path changes at 30s from AIR1 to AIR2.

Table 1. Comparison of PESQ score for different algorithms

Algorithm	PESQ
FDAF-PEM_AFC (with $\mu = 0.001$)	2.51
FDAF-PEM_AFC (with $\mu = 0.02$)	3.17
PBFDFAF-PEM-AFC (with $\mu = 0.001$)	2.69
PBFDFAF-PEM-AFC (with $\mu = 0.02$)	3.36
OSS-FDAF-PEM-AFC	4.16
OSS-PBFDFAF-PEM-AFC	4.27

Table 2. Computational complexity analysis of OSS-FDAF-PEM_AFC algorithm

Algorithm 1. OSS-FDAF-PEM-AFC	No. of real multiplications required
$\hat{\Phi}_{u_f, m}(0) = \Phi_{e_f, m}(0) = [0]_{N \times 1}$; $\hat{A}(q, l) = [1, 0_{n_A-1}]^T$	
$n_w = R, N = 2R$	
$u(l) = [u(lR - M + 1) \dots u(lR - 1), u(lR)]^T$,	
$\hat{W}(l) = \mathcal{F}[\hat{W}^T, 0_{1 \times N}]^T = [\hat{W}_{l,0}(l), \dots, \hat{W}_{2N-1}(l)]^T$	$N \log_2 N$
$\tilde{s}(l) = \mathcal{F}_N^{-1}\{U(l)\hat{W}(l)\}$	$3N + N \log_2 N$
$e(l) = s(l) - \hat{s}(l)$	

$$\begin{aligned}
 \mathbf{u}_f(l) &= \begin{bmatrix} \hat{A}(q,l)\mathbf{u}(lR-N+1) \\ \mathbf{M} \\ \hat{A}(q,l)\mathbf{u}(lR) \end{bmatrix} = [u_f(lR-N+1) \dots u_f(lR-1), u_f(lR)]^T & Nn_A \\
 \mathbf{U}_f(l) &= \text{diag}\{\mathcal{F}\mathbf{u}_f(l)\} = \text{diag}\{[U_{f0}(l), U_{f1}(l), \dots, U_{f(2N-1)}(l)]^T\} & N \log_2 N \\
 \mathbf{s}_f(l) &= \begin{bmatrix} \hat{A}(q,l)s(lR-R+1) \\ \mathbf{M} \\ \hat{A}(q,l)s(lR) \end{bmatrix} = [s_f(lR-R+1) \dots s_f(lR-1), s_f(lR)]^T & Rn_A \\
 \mathbf{S}_f(l) &= \mathcal{F}[0_{1 \times N}, s_f(lN), \dots, s_f(lN+N-1)]^T & N \log_2 N \\
 \mathbf{E}_f(l) &= \mathbf{S}_f(l) - \mathcal{G}^{01} \mathbf{U}_f \hat{\mathbf{w}}(l) & 2N \log_2 N + 3N \\
 \hat{\Phi}_{u_f,m}(l) &= \lambda \hat{\Phi}_{u_f,m}(l-1) + (1-\lambda) |U_{f,m}(l)|^2, & 5N \\
 \Lambda(l) &= \text{diag}\{[\Phi_{u_f,0}(l), \dots, \Phi_{u_f,2N-1}(l)]^T\} \\
 \Phi_{e_f,m}(l) &= \alpha \Phi_{e_f,m}(l-1) + (1-\alpha) |E_{f,m}(l)|^2; \Phi_{x,m}(l) = \Phi_{e_f,m}(l) & 5N \\
 \mu_m(l) &= \frac{\Phi_{u_f,m}(l)\delta_m(l)}{\Phi_{u_f,m}(l)\delta_m(l) + 2\Phi_{x,m}(l)} & 14N \\
 \dot{W}(l+1) &= \dot{W}(l) + \mathcal{G}^{10} \mu_m(l) \Lambda^{-1}(l) \mathbf{U}_f^H(l) \mathbf{E}_f(l) & 2N \log_2 N + 15N \\
 \Theta_m(l+1) &= |\hat{W}_m(l+1) - \hat{W}_m(l)|^2 & 2N \\
 \delta_m(l+1) &= \left(1 - \frac{\mu_m(l)}{4}\right) \delta_m(l) + \Theta_m(l+1) & 5N \\
 \hat{A}(q,l) &= \text{levinson-durbin}\{e(l); e(l-1)\} & n_A^2 + (5+N)n_A + N
 \end{aligned}$$

Total Complexity in terms of no of multiplications required per sample: $(8N \log_2 N + 53N + (2N + R + 5)n_A + n_A^2) / R$

Table 3. Computational complexity analysis of OSS-PBFDAF-PEM_AFC algorithm

Algorithm 2. OSS-PBFDAF-PEM-AFC	No. of real multiplications required
$\hat{\Phi}_{u_f,m}(0) = \Phi_{e_f,m}(0) = [0]_{N \times 1}$, $\hat{A}(q,l) = [1, 0_{n_A-1}]^T$ $R = \frac{n_W}{P}$, $N = 2R$ for $l = 0, 1, \dots$ do for $p = 0, 1, \dots, P-1$ do $\mathbf{u}_p(l) = [u(lR - (p+1)N + 1) \dots u(lR - pN - 1), u(lR - pN)]^T$,	

$$U_p(l) = \text{diag}\{\mathcal{F}_N \mathbf{u}_p(l)\} = \text{diag}\{[U_{p0}(l), U_{p1}(l), \dots, U_{p(2N-1)}(l)]^T\} \quad PN \log_2 N$$

end for

$$\hat{s}(l) = \mathcal{F}_N^{-1} \sum_{p=0}^{P-1} U_p(l) \hat{w}_p(l) \quad PN \log_2 N + 3PN$$

$$e(l) = s(l) - \hat{s}(l)$$

for $P = 0, 1, \dots, P-1$ do

$$\mathbf{u}_{fp}(l) = \begin{bmatrix} \hat{A}(q, l) \mathbf{u}(lR - (p+1)N + 1) \\ \mathbf{M} \\ \hat{A}(q, l) \mathbf{u}(lR - pN) \end{bmatrix} = [u_f(lR - (p+1)N + 1) \dots u_f(lR - pN)]^T \quad PN n_A$$

$$U_{fp}(l) = \text{diag}\{\mathcal{F}_N \mathbf{u}_{fp}(n)\} = \text{diag}\{[U_{fp,0}(l), U_{fp,1}(l), \dots, U_{fp,(2N-1)}(l)]^T\} \quad PN \log_2 N$$

$$s_f(l) = \begin{bmatrix} \hat{A}(q, l) s(lR - R + 1) \\ \mathbf{M} \\ \hat{A}(q, l) s(lR) \end{bmatrix} = [s_f(lR - R + 1) \dots s_f(lR - 1), s_f(lR)]^T \quad PR n_A$$

$$S_f(l) = \mathcal{F}[0_{1 \times N}, s_f(lN), \dots, s_f((l+1)N - 1)]^T \quad PN \log_2 N$$

end for

$$E_f(l) = S_f(l) - \mathcal{G}^{01} \sum_{p=0}^{P-1} U_{f,p}(l) \hat{w}_p(l) \quad 2PN \log_2 N + 3PN$$

for $P = 0, 1, \dots, P-1$ do

$$\hat{\Phi}_{u_{fp},m}(l) = \lambda \hat{\Phi}_{u_{fp},m}(l-1) + (1-\lambda) |U_{fp,m}(l)|^2 \quad 5PN$$

$$\ddot{E}_p(l) = \text{diag}\{[\Phi_{u_{fp},0}(l), \dots, \Phi_{u_{fp},2N-1}(l)]^T\}$$

$$\Phi_{e_f,m}(l) = \alpha \Phi_{e_f,m}(l-1) + (1-\alpha) |E_{f,m}(l)|^2 ; \Phi_{x,m}(l) \approx \Phi_{e_f,m}(l) \quad 5PN$$

$$\mu_{p,m}(l) = \frac{\Phi_{u_f,m}(l) \delta_{p,m}(l)}{\Phi_{U_{fp},m}(l) \left[\delta_{p,m}(l) + \frac{1}{2} \sum_{p=0, m \neq p}^{P-1} \delta_{p,m}(l) \right] + 2\Phi_{x,m}(l)} \quad 16PN$$

$$\dot{W}_p(l+1) = \dot{W}_p(l) + \mathcal{G}^{10} \mu_{p,m}(l) \Lambda^{-1}(l) U_{fp}^H E_f(l) \quad 2PN \log_2 N + 15PN$$

$$\delta_{p,m}(l+1) = \left[1 - \frac{\mu_{p,m}(l)}{2} + \frac{\mu_{p,m}^2(l)}{4} \right] \delta_{p,m}(l) + \frac{1}{8} \mu_{p,m}^2(l) \\ \times \sum_{p=0, m \neq p}^{P-1} \delta_{p,m}(l) + \frac{1}{2} \mu_{p,m}^2(l) \frac{\Phi_{x,m}(l)}{\Phi_{u_f,m}(l)}, \quad 23PN$$

end for

$$\hat{A}(q, l+1) = \text{levinson-durbin}\{e(l); e(l-1)\} \quad n_A^2 + (5+N)n_A + N$$

end for

Total Complexity in terms of no of multiplications required per sample :

$$(8PN \log_2 N + 70PN + N + (PN + PR + 5 + N)n_A + n_A^2) / R$$

Table 4. Comparison of computational complexity

Algorithm	Computational Complexity	No. Multiplications per sample		
FDAF-PEM_AFC	$(8N \log_2 N + 27N + (2N + R + 5)n_A + n_A^2) / R$	249		
PBFDAF-PEM-AFC	$(8PN \log_2 N + 44PN + N + (PN + PR + 5 + N)n_A + n_A^2) / R$	285 (P=1)	507 (P=2)	919 (P=4)
OSS-FDAF-PEM-AFC	$(8N \log_2 N + 53N + (2N + R + 5)n_A + n_A^2) / R$	302		
OSS-PBFDAF-PEM-AFC	$(8PN \log_2 N + 70PN + N + (PN + PR + 5 + N)n_A + n_A^2) / R$	286 (P=1)	612 (P=2)	1128 (P=4)

The comparison of computational complexity of discussed algorithms is presented in Table 3. It has been noticed that the OSS algorithms requires only few additional multiplication operations compared to fixed step-size algorithms. Among the proposed two algorithms OSS-FDAF-PEM-AFC algorithm has lower computational load compared to OSS-PBFDAF-PEM-AFC. But, the processing delay of frequency domain adaptive filter is given by $(2R-1)$, where R is the frame shift. Hence, the processing delay of FDAF is $(n_w - 1)$ and for

PBFDAF is $(\frac{n_w}{P} - 1)$, where n_w is length of adaptive filter and P is no of partitions. Thus, even though OSS-PBFDAF-PEM-AFC algorithm has slightly higher computational load, it may be preferred due to its low processing delay.

6. CONCLUSIONS

In this paper, we proposed a robust optimal step-size technique for FDAF and PBFDAF algorithms for PEM-AFC configuration. Computer simulation indicated that the OSS algorithms have good performance in faster convergence and low steady-state error compared to fixed step size algorithms, but the computational complexity of OSS algorithms is slightly higher. Among the two proposed algorithms, OSS-FDAF-PEM-AFC has better performance than the OSS-PBFDF-PEM-AFC algorithm in terms of faster convergence, misalignment, and low computational complexity. However, hearing aid devices demand low processing delay, in such case OSS-PBFDAF-PEM-AFC may be preferred over the OSS-FDAF-PEM-AFC algorithm, even though its computational complexity is slightly higher.

REFERENCES

1. Kates, J.M. Digital hearing aids. Plural Publishing, San Diego, CA, 2008.
2. Spriet, A.; Rombouts, G.; Moonen, M. & Wouters, J. Feedback control in hearing aids., *In Handbook of speech processing*, edited by J. Benesty, M.M. Sondhi & Y.A. Huang. Springer, Berlin, Heidelberg, 2008. pp. 979-1000. doi: 10.1007/978-3-540-49127-9_48
3. Siqueira, M.G. & Alwan, A. Steady-state analysis of continuous adaptation in acoustic feedback reduction systems for hearing-aids. *IEEE Trans. on Speech and Audio Process.*, 2000, **8**(4), 443-453.

doi: 10.1109/89.848225

4. Vasundhara; Panda, G. & Puhan, N.B. An improved block adaptive system for effective feedback cancellation in hearing aids. *Digital Signal Process.*, 2016, **48**, 216-225. doi: 10.1016/j.dsp.2015.08.016
5. Paleologu, C.; Ciocchina, S; & Benesty, J. An overview on optimized NLMS algorithms for acoustic echo cancellation. *EURASIP J. Adv. Signal Process.*, 2015, **97**. doi: 10.1186/s13634-015-0283-1
6. Boukis, C.; Mandic, D.P. & Constantinides, A.G. Bias reduction in acoustic feedback cancellation systems with varying all-pass filters. *Electron. Lett.*, 2006, **42**(9), 556-558. doi: 10.1049/el:20060470
7. Ngo, K.; Van Waterschoot, T.; Christensen, M.G.; Moonen, M. & Jensen, S.H. Improved prediction error filters for adaptive feedback cancellation in hearing aids. *Signal Process.*, 2013, **93**(11), 3062-3075. doi: 10.1016/j.sigpro.2013.03.042
8. Akhtar, M.T.; Albu, F. & Nishihara, A. Acoustic feedback cancellation in hearing aids using dual adaptive filtering and gain-controlled probe signal. *Biomedical Signal Process. and Control*, **52**, 1-13. doi: 10.1016/j.bspc.2019.03.012
9. Albu, F.; Tran, L. T. & Nordholm, S. A combined variable step size strategy for two microphones acoustic feedback cancellation using proportionate algorithms. *In Asia-Pacific Signal and Information Process. Association Annual Summit and Conf.*, IEEE, 2017, 1373-1377. doi: 10.1109/APSIPA.2017.8282247
10. Schneider, M. & Kellermann, W. The generalized frequency-domain adaptive filtering algorithm as an approximation of the block recursive least-squares algorithm. *EURASIP J. Adv. Signal Process.*, 2016, **1**, 1-15. doi: 10.1186/s13634-015-0302-2
11. Pradham, S.; George, N.V.; Albu, F. & Nordholm, S. Two microphone acoustic feedback cancellation in digital hearing aids: A step size controlled frequency domain approach. *Appl. Acoust.*, 2018, **132**, 142-151. doi: 10.1016/j.apacoust.2017.11.015
12. Yang, F.; Enzner, G. & Yang, J. Statistical convergence analysis for optimal control of dft-domain adaptive echo

- canceler. *IEEE/ACM Trans. on Audio, Speech, and Lang. Process.*, 2017, **25**(5), 1095-1106.
doi: 10.1109/TASLP.2017.2671422
13. Prasad, S.S. & Rao, C.B. Acoustic feedback cancellation using optimal step-size control of the partition block frequency-domain adaptive filter. In *Advances in communications, signal processing, and VLSI: Lecture notes in electrical engineering*, Springer, 2021, **722**, 139-151.
doi: 10.1007/978-981-33-4058-9_13
 14. Bernardi, G.; Waterschoot, T.V.; Wouters, J. & Moonen, M.M. A PEM-based frequency-domain kalman filter for adaptive feedback cancellation. In *23rd European Signal Processing Conf., IEEE*, 2015, 270-274.
doi: 10.1109/EUSIPCO.2015.7362387
 15. Dutta, S.C.; Gopinathan, E. & Patney, R.K. Digital filters using identical blocks. *Def. Sci. J.*, 2014, **35**(3), 267-280.
doi: 10.14429/dsj.35.6021
 16. Yang, F. & Yang, J. Optimal step-size control of the partitioned block frequency-domain adaptive filter. *IEEE Trans. on Circuits and Systems II: Express Briefs*, 2017, 814-818.
doi: 10.1109/TCSII.2017.2780880
 17. Yang, F.; Wu, M. & Yang, J. A computationally efficient delayless frequency-domain adaptive filter algorithm. *IEEE Trans. on Circuits and Systems II: Express Briefs*, 2013, **60**, 222-226.
doi: 10.1109/TCSII.2013.2240877
 18. Vasundhara; Panda, G & Puhan, N.B. A low complexity delayless frequency domain feedback canceller for hearing aids. *IEEE Int. Symposium on Signal Process. and Information Technology (ISSPIT)*, 2015, 157-162.
doi: 10.1109/ISSPIT.2015.7394319.
 19. Sankowsky, R.T.; Blau, M.; Schepker, H. & Doclo, S. Reciprocal measurement of acoustic feedback paths in hearing aids. *J. Acoust. Soc Am*, 2015, 399-404.
doi: 10.1121/1.4933062
 20. Bernardi, G.; Waterschoot, T.V.; Wouters, J. & Moonen, M. Adaptive feedback cancellation using a partitioned-block frequency-domain kalman filter approach with pem-based signal prewhitening. *IEEE/ACM Trans. on Audio, Speech, and Lang. Process.*, 2017, **25**, 1784-1798.
doi: 10.1109/TASLP.2017.2716188
 21. Loizou, P.C. *Speech enhancement: Theory and practice*. CRC press, 2013.
doi: 10.1201/9781420015836

CONTRIBUTORS

Mr S. Siva Prasad received BTech Degree in Electronics and Communications Engineering, from JNTU Hyderabad, and MTech in Microelectronics and VLSI design from NIT Calicut. He is currently pursuing Phd in the area of improved algorithms for acoustic feedback cancellation at NIT Warangal. His research areas of interest are Adaptive Signal Processing, Bio Medical Signal Processing, DSP Architectures and Algorithms.

In the current study, he came up with the concept, conducted the literature review, and completed the simulation work, which included the interpretation and analysis of the results.

Prof. C.B. Rama Rao earned his Bachelor and Master degrees from JNTU Kakinada and his PhD from IIT Kharagpur. He is currently employed as a professor at NIT Warangal's Department of Electronics and Communication Engineering. Adaptive signal processing, musical instrument signal processing, voice signal processing, and biomedical signal processing were amongst his main research interests. He has around 35 papers published in reputed journals and conferences.

In the current study, he gave the idea, examined the work, validated the results, provided the guidance, and made other helpful insights.